Blue-Shifted and Red-Shifted Hydrogen Bonds in Hypervalent Rare-Gas FRg−H···Y Sandwiches

Igor V. Alabugin* and Mariappan Manoharan

Department of Chemistry and Biochemistry, Florida State University, Tallahassee, Florida 32306-4390

Frank A. Weinhold

Theoretical Chemistry Institute, Department of Chemistry, University of Wisconsin-Madison, Madison, Wisconsin 53706

Increased $F^-[Rg-H]^+$ resonance contribution provides an efficient mechanism for the Rg−H bond repolarization in the hypervalent 3c,4e−F−Rg−H···Y complexes, where Rg is a rare gas atom. This effect which parallels the effect of rehybridization in classic 2c,2e chemical bonds, decreases the population of the $\sigma^*(Rg-H)$ orbitals and increases the covalent Rg−H bond order leading to Rg−H bond contraction. The origin of this electronic reorganization can be ascribed to competition of two hyperconjugative donors for the same $\sigma^*(Rg-H)$ acceptor. As donor Y approaches the H atom of an FRgH moiety, the $n(Y) \rightarrow \sigma^*(H-Rg)$ interaction becomes stronger, whereas the $n(F) \rightarrow \sigma^*(Rg-H)$ interaction becomes weaker in an asynchronous process. For weaker donors Y and longer Y···H distances, breaking of the Rg−F covalent bond proceeds faster than formation of the H−Y bond. As a result, both the $\sigma^*(Rg-H)$ population and the Rg−H distance decrease thus accounting for the blue-shift in such H-bonded complexes. However, when Y is a moderately strong donor and/or when $\sigma^*(Rg-H)$ is a very strong acceptor, a further decrease in Y···H distance leads to the formation of a sigma bond with the incoming donor (Y) in an S_N2-like process with concomitant elimination of the fluoride moiety. As a result, the F−Rg−H···Y systems are transformed into dissociated $F^-···Rg···[HY]^+$ complexes, and a large Rg−H elongation and red shift are observed.

Introduction

The unusual phenomenon of "blue-shifted" or "improper" X−H···Y hydrogen bonding[1] which is accompanied by X−H bond contraction and a blue shift of the X−H IR stretching frequency continues to receive significant experimental[2−4] and theoretical[5,6] attention. Recently, we showed that the direction of the X−H bond structural reorganization is determined by the balance of two opposing effects: X−H bond lengthening due to hyperconjugative $n(Y) \rightarrow \sigma^*(X-H)$ interaction and X−H bond shortening due to the increase in hydrogen electropositivity and polarization of X−H bonds.[7] Under favorable conditions when the $n(Y) \rightarrow \sigma^*(X-H)$ hyperconjugative interaction is weak and the X-hybrid orbital in the X−H bond is capable of sufficient changes in polarization and hybridization, this collection of effects leads to the X−H bond contraction and to the blue-shift of the X−H stretching frequency.

Even though the increase in X−H bond polarization is a key factor in the process of H-bond formation, it can lead to X−H bond contraction only when a suitable avenue for the structural reorganization is available. In the case of normal 2c,2e bonds, such an avenue is provided by rehybridization[8] as a direct consequence of Bent's rule.[9] The rehybridization model provided explanations for a number of puzzling experimental and theoretical findings and led to the computational discovery of new types of blue-shifted H-bonds including the first blue-shifted RO−H···Y H complexes.

However, the bond rehybridization concept is not applicable to atoms that lack the valence p-shell vacancies needed for effective hybrid formation, notably closed-shell rare gas (Rg) atoms. As a result, one cannot use the rehybridization model for analysis of H bonding in a recently discovered new class of hypervalent complexes of HArF and HKrF molecules, which are found to be blue-shifted.[10,11] Computational evidence suggests that the same is true for H-bonded FRgH complexes with Rg = He, where the closed-shell $(1s)^2$ character is even more inimical to hybridization.[12] Summarizing available experimental and theoretical observations, Lignell et al. arrived at the remarkable conclusion that "for these rare gas containing compounds the blue shift of the H−Rg stretching vibration is a normal effect".[13]

The unusual H-bonding properties of these compounds presumably reflect the unusual features of 3c-4e bonding in hypervalent molecules which has fascinated chemists for a long time.[14−17] Since the number of bonds at the central atoms apparently exceeds that allowed by the octet rule,[18] the involvement of d orbitals was initially considered to be of primary importance[19] but was shown subsequently to be limited to providing adequate polarization functions rather than being "true participants in hybridization".[20] Usually, hypervalent bonding is described by the molecular orbital (MO) model of Rundle[21] and Pimentel[22−24] (Figure 1) or 3-center-4-electron (3c-4e) bonds of valence bond (VB) theory which treats such compounds as resulting from a superposition of resonance structures each of which does not violate the octet rule. For example, XeF_2 is

---

* To whom correspondence should be addressed. E-mail: alabugin@chem.fsu.edu.

Hypervalent Rare-Gas FRg−H···Y Sandwiches

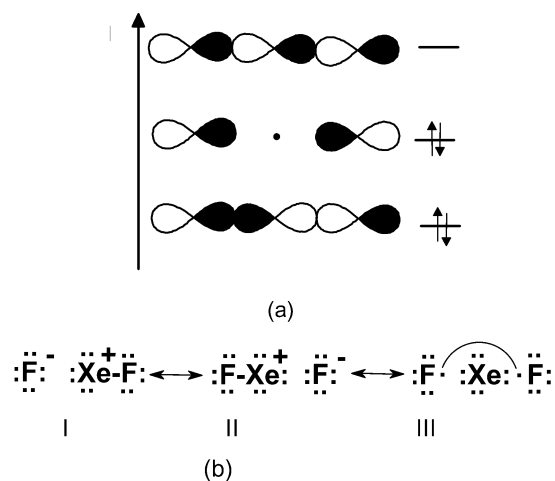*J. Phys. Chem. A, Vol. 108, No. 21, 2004* **4721**

(a)

(b)

Figure 1. MO (a) and VB (b) descriptions of 3c-4e bonding in XeF$_2$.

described through a resonance of two partially ionic VB structures (I) and (II) and a long bond structure, (III) (Figure 1).[24−27]

In this paper, we will show how the nature of chemical bonding in hypervalent systems provides a novel mechanism for electronic and structural reorganization during H-bonding. We will begin with a discussion of the general factors associated with a dynamic electronic reorganization in the process of the F−He−H···N$_2$ complex formation, proceed further with analysis of structural and electronic changes for a larger number of F−Rg−H···Y H-bonded complexes, and conclude with a comparison of blue-shifted H-bonds in hypervalent systems with blue-shifted H-bonds in classic 2c,2e systems.

Computational Details and Choice of Method

All computations were performed using the Gaussian 98 program[28] at the MP2(FC) and B3LYP levels of theory with extended basis sets (cc-pVDZ, cc-pVTZ, 6-311++G(d,p), 6-311++G(2d,2p). Zero-point vibrational energy (ZPE) and counterpoise corrections[29] were applied to the interaction energies. Binding energies of three FRgH···N$_2$ complexes were also evaluated at CCSD(T)/6-311++G(2d,2p) level of theory. The scan computations were done by freezing the H···Y distance using opt=Modredundant option in Gaussian 98 and optimizing all other structural parameters. The NBO 4.0[30] program was used to analyze electronic changes upon formation of H-bonded complexes. The NBO analysis transforms the canonical delocalized MOs into localized orbitals that "are closely tied to chemical bonding concepts". Detailed descriptions of the NBO calculations are available.[31,32] For all NBO computations, the option "density=MP2" was used to analyze the higher-level

corrections to the HF density. The second order perturbation energies were obtained directly from the HF wave function.

Results and Discussion

Dynamics of Structural and Electronic Changes in the Process of F−He−H···N$_2$ Complex Formation. In the first section, we will discuss the electronic and structural reorganization that accompanies the formation of H-bonds with FHeH, the smallest of the FRgH molecules, as an illustrative example. We will monitor the dynamic electronic reorganization in the F−He−H moiety upon the collinear approach of a nitrogen molecule. During this process, the H···N distance is scanned between 4.7 and 1.5 Å while all other variables are optimized.

Structural Changes. The Rg−H bond begins to shorten and the F−Rg bond starts to elongate as the H-bond acceptor approaches the hydrogen atom more closely than 3 Å. Although the F−He distance continues to increase steadily even at shorter H···N distances, the trend for the He−H bond reverses when the system approaches the equilibrium geometry where the He−H distance starts to *increase*. Interestingly, all of these changes are qualitatively *analogous* to those observed for the 2c,2e bonds in the CF$_3$H···H$_2$O complex (Figure 2). As far as quantitative differences between the two complexes are concerned, the following two are noteworthy: (a) changes in the F−He bond length are significantly larger than changes in the C−F distances and (b) the observed change from blue- to red-shifted H-bonding occurs at much shorter H···Y distances in the hypervalent system.

This analysis is consistent with earlier observations of McDowell, who after comparing rare gas H-bonded complexes with complexes of "normal" molecules with the same acceptor concluded that hypervalent rare gas molecules are much more perturbed by the same donor than "normal molecules (e.g., HKrCl vs HCl)[10a] and suggested that the observed blue shift can be explained through a combination of charge transfer (hyperconjugation) and electrostatic effects. We will analyze these effects in detail in the next section.

Electronic Changes. The Balance of n(F) → σ*(He−H) and n(N) → σ*(H−He) Interactions, "He-Bonding" vs "H-Bonding". An insight into the origin of blue-shifted H-bonding in hypervalent systems is given in Figure 3 which compares the effect of H···N distance changes on the magnitudes of n(F) → σ*(He−H) and n(N) → σ*(H−He) interactions. The first interaction is extremely strong in the isolated FHeH where it corresponds to one of the major VB structures contributing to the 3c,4e bond (vide infra) and solely accounts for the covalent component of He−F bonding. He−H$^+$ is a strongly bound ion isoelectronic to H$_2$,[33,34] and one can consider FHeH as a F$^−$···[He−H$^+$] type complex bound through a
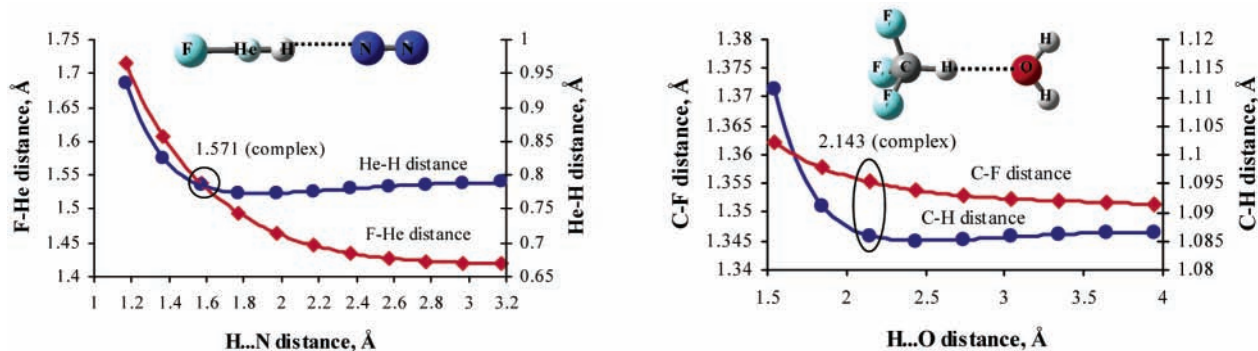

Figure 2. Correlation of H···N distance with F−He and He−H bond lengths in FHeH···N$_2$ complex (on the left) and correlation of H···O distance with F−C and C−H bond lengths in F$_3$CH···OH$_2$ complex (on the right). The equilibrium distances in the complexes are circled.
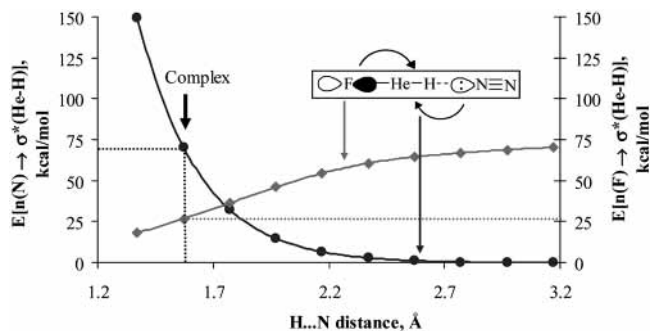
Figure 3. Correlations of H$\cdots$N bond length in FHeH$\cdots$N$_2$ complex with energies of the n → σ^* hyperconjugative interactions at the MP2/6-311++G(2d,2p) level (n(F) → σ^*(He−H) interaction, diamonds, n(N) → σ^*(H−He) interaction, circles).
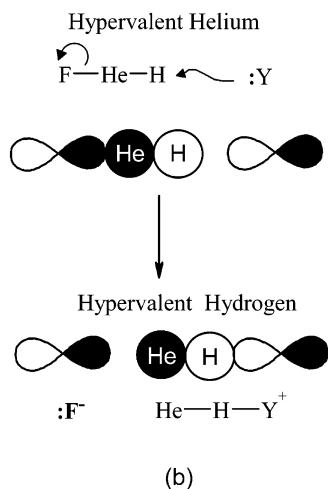

(b)

Figure 4. Transition from "He-bonding" to H-bonding in the process of FHeH$\cdots$Y complex formation.

combination of hyperconjugative and ionic interactions which perfectly fit all of the attributes of strong H-bonding with the only difference that they involve a helium rather than a hydrogen atom. In analogy to H-bonding, this phenomenon can be called "He-bonding". As the H$\cdots$N distance decreases, the magnitudes of the n(F) → σ^*(He−H) interaction and covalent F−He bonding decrease, whereas the ionic F$^-$$\cdots$[He−H]$^+$ bond order increases, features indicating an increase in the F$^-$$\cdots$[He−H]$^+$ character. On the other hand, the n(N) → σ^*(H−He) interaction increases steadily until, at the shorter N$\cdots$H distances, it reaches the magnitude of a weak covalent bond indicating proton transfer to the nitrogen molecule. The structure of the F−He−H$\cdots$N$_2$ complex can be best described as a F$^-$$\cdots$He−H$^+$$\cdots$ N$_2$ sandwich of the positively charged diatomic cation [He−H]$^+$ with two hyperconjugative donors where the nature of the attractive interactions between [He−H]$^+$ of the cation with the donors is very similar at the hydrogen end (classic H-bonding) and at the helium end (more esoteric "He-bonding", Figure 4). The relative magnitudes of n(F) → σ^*(He−H) and n(N) → σ^*(H−He) interactions give an indication of the relative weights of [F−Rg]$^+$H$^-$ and [Rg−H]$^+$F$^-$ VB structures (the later VB structure will be transformed into F$^-$$\cdots$Rg$\cdots$[H−Y]$^+$ at the later stages).

Even though for the extremely strong hyperconjugative interactions in Table 2 and Figure 3 the second-order perturbation n(Y) → σ^*(He−H) energies should be taken only for qualitative comparisons,[35] they still provide an insight into the nature of electronic changes that accompany H-bond formation. A decrease in n(F) → σ^*(He−H) interaction leads to a decrease in the σ^*(He−H) population, whereas an increase in the n(N)

→ σ^*(H−He) interaction has the opposite effect. The net change in the σ^*(He−H) population and the ultimate direction of the Rg−H bond length change depend on the balance of these two interactions which changed in an antiparallel way. Because at the longer Y$\cdots$H distances the n(F) → σ^*(Rg−H) interaction weakens faster than n(Y) → σ^*(H−Rg) increases in magnitude, a seemingly paradoxical decrease in the population of the σ^*(H−Rg) orbital is observed initially, an effect which is just the opposite of that found for both blue and red-shifted H-bonding involving classic 2c,2e X−H bonds.[7]

From a slightly different perspective, H-bonding in this system can be described as a competition of two hyperconjugative donors for the same σ^*(He−H) acceptor, a process analogous to an S$_N$2 reaction where bonding of the central carbon with an incoming nucleophile results in breaking of the covalent bond with a leaving group. This analogy is further enhanced by the analogous nodal structures of an antibonding σ^*(He−H) orbital and a p orbital on the hypervalent central carbon atom in the TS for an S$_N$2 reaction (Figure 5).

Molecular and Atomic Charges. In full agreement with the above picture, there is no charge transfer between Y and the F−Rg−H moiety at the 3−2.2 Å region where the factors behind the structural reorganization are mostly electrostatic. However, an increasing amount of electron density is transferred from N$_2$ to HHeF at the shorter H$\cdots$Y distances as the result of a hyperconjugative n(N) → σ^*(Rg−H) interaction.
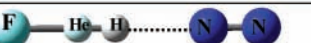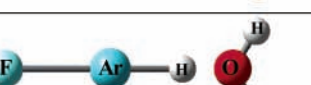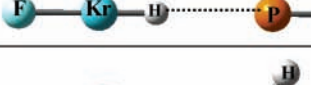
Initially, charges at the terminal atoms of the F−He−H moiety change in opposite directions, the hydrogen atom becomes more positive while the fluorine atom becomes more negative (Figure 6). Interestingly, the atomic charge of He barely changes at this range; the He atom can be considered merely a transmitting point for the density redistribution between the F and H atoms. However, at N$\cdots$H distances of 1.8−1.6 Å where the two curves in Figure 3 intersect and a switch from "He-bonding" to H-bonding is observed, the situation changes and the positive charge at the H atom starts to decrease while the He atom begins to acquire a progressively larger positive charge.

These results are in a good agreement with recent observations in the literature. For example, Lignell and co-workers found that the charge of the HKr unit in HKrCl increased in the linear complex with N$_2$ compared to that in the isolated molecule and that electrostatic forces provide the most important contribution in linear HArF$\cdots$N$_2$,[13] HKrF$\cdots$N$_2$,[13] and HKrCl$\cdots$N$_2$[11,13] complexes according to the Morokuma interaction energy decomposition scheme. Nemukhin et al. reported that the partial charge of the Xe−H moiety increases as the Xe−H bond shortens in HXeOH−(H$_2$O) complexes.[36] McDowell has shown that the H atom becomes more positive, whereas the Rg and F atoms become more negative in the process of H-bond formation in FRgH$\cdots$Y complexes,[10] an effect which was modeled reasonably well with point charges.

Bond Polarization and Population of the σ^*(He−H) Orbital. Notwithstanding the above changes in the atomic charges, the Rg−H bond polarization steadily increases as the H$\cdots$N distance decreases below 3 Å, a trend analogous to that observed for 2c,2e bonds such as C−H bond in CF$_3$H$\cdots$OH$_2$ complex (Figure 7).

Another interesting trend is observed for the population of the σ^*(He−H) orbital which decreases initially but starts to increase when the N$\cdots$H distances fall below 1.7 Å. This initial decrease in the σ^*(He−H) population is the first significant difference from the behavior observed for 2c,2e X−H bonds (compare it with the changes in the population of σ^*(C−H)

Hypervalent Rare-Gas FRg−H···Y Sandwiches

J. Phys. Chem. A, Vol. 108, No. 21, 2004 **4723**

TABLE 1: Structural Parameters Associated with the Formation of H-Bonded Complexes of Rare-Gas Compounds (FRgH, Rg = He, Ar, and Kr) with OC, CO, N_2, P_2, H_2O, NH_3 at the MP2 Level with 6-311++G(d,p) and 6-311++G(2d,2p) Basis Sets[a]

FRgH...Y	BS	Å	Å	Å	Å
F–He–H	6-311++G(d,p)	1.4037	0.8228	-	-
	6-311++G(2d,2p)	1.4130	0.7930	-	-
F–He–H ···· O–C	6-311++G(d,p)	1.4240	0.8006	2.1766	-0.0222
	6-311++G(2d,2p)	1.4562	0.7706	1.8887	-0.0224
F–He–H ···· C–O	6-311++G(d,p)	1.8490	1.1158	1.1802	0.2930
	6-311++G(2d,2p)	1.8038	1.0735	1.1985	0.2805
F–He–H ···· N–N	6-311++G(d,p)	1.5855	0.8217	1.4481	-0.0010
	6-311++G(2d,2p)	1.5380	0.7854	1.5710	-0.0076
F–He–H ···· P–P	6-311++G(d,p)	1.6137	0.9141	1.7352	0.0913
	6-311++G(2d,2p)	1.5398	0.8291	1.9200	0.0361
F–He–H ···· O(H,H)	6-311++G(d,p)	1.8763	1.0947	1.0344	0.2719
	6-311++G(2d,2p)	1.8439	1.0783	1.0365	0.2853
F–Ar–H	6-311++G(d,p)	2.0490	1.3296	-	-
	6-311++G(2d,2p)	1.9980	1.3254	-	-
F–Ar–H ···· O–C	6-311++G(d,p)	2.0726	1.3161	2.3218	-0.0135
	6-311++G(2d,2p)	2.0128	1.3154	2.2899	-0.0100
F–Ar–H ···· C–O	6-311++G(d,p)	2.1570	1.3267	1.8807	-0.0029
	6-311++G(2d,2p)	2.0681	1.3237	1.9637	-0.0017
F–Ar–H ···· N–N	6-311++G(d,p)	2.0962	1.3126	2.1318	-0.0170
	6-311++G(2d,2p)	2.0281	1.3151	2.1637	-0.0103
F–Ar–H ···· P–P	6-311++G(d,p)	2.1052	1.3334	2.3309	0.0038
	6-311++G(2d,2p)	2.0380	1.3348	2.3447	0.0094
F–Ar–H ···· O(H,H)	6-311++G(d,p)	2.4054	1.5574	1.1249	0.2278
	6-311++G(2d,2p)	2.3372	1.5930	1.1112	0.2676
F–Kr–H	6-311++G(d,p)	2.0739	1.4800	-	-
	6-311++G(2d,2p)	2.0725	1.4709	-	-
F–Kr–H ···· O–C	6-311++G(d,p)	2.0795	1.4745	2.6034	-0.0055
	6-311++G(2d,2p)	2.0806	1.4642	2.5046	-0.0067
F–Kr–H ···· C–O	6-311++G(d,p)	2.0973	1.4724	2.4734	-0.0076
	6-311++G(2d,2p)	2.1039	1.4637	2.3284	-0.0072
F–Kr–H ···· N–N	6-311++G(d,p)	2.0870	1.4730	2.4886	-0.0070
	6-311++G(2d,2p)	2.0878	1.4638	2.4465	-0.0071
F–Kr–H ···· P–P	6-311++G(d,p)	2.0876	1.4795	2.7761	-0.0005
	6-311++G(2d,2p)	2.0917	1.4724	2.6281	0.0015
F–Kr–H ···· O(H,H)	6-311++G(d,p)	2.1654	1.4766	1.7350	-0.0034
	6-311++G(2d,2p)	2.1601	1.4694	1.7425	-0.0015
F–Kr–H ···· N(H,H,H)	6-311++G(d,p)	2.5531	2.0414	1.0685	0.5614
	6-311++G(2d,2p)	2.5066	2.0121	1.0687	0.5412

[a] See the Supporting Information for the DFT and other MP2 results.

orbital in CF_3H···OH_2 complex in Figure 8). This difference between the two types of blue-shifted H-bonded systems is noteworthy because in both cases an increasing amount of electron density is transferred to the H-bond donor from the H-bond acceptor Y as it approaches the hydrogen atom.

Remarkably, the trends given in Figures 6 and 8 change their direction at the same critical region of 1.7−1.8 Å where the curves for the energies of n(F) → σ*(He−H) and n(N) → σ*(H−He) interactions in Figure 3 intersect. Clearly, the decrease in the σ*(He−H) population results from the faster decrease in the magnitude of n(F) → σ*(He−H) interaction as a result of competing n(N) → σ*(H−He) interaction. Unlike in

the case of H-bonding in classic 2c,2e X−H-bonds, increased n(Y) → σ*(X−H) hyperconjugation *contributes* (albeit in an indirect way) to the blue shift in "hypervalent" H-bonds!

Structural Changes Associated with H-Bond Formation in Other F−Rg−H···Y Systems. Most of the trends discussed in the previous sections are also observed for other H-bonded F−Rg−H···Y complexes. Calculated geometries of isolated F−Rg−H molecules and respective F−Rg−H···Y compounds, where Y = N_2, CO, OC, P_2, NH_3, and water, are given in Table 1. Some of the complexes with P_2 were recently reported to be red-shifted,[10f] whereas the complexes with water and ammonia have not been reported before. The first three complexes are

TABLE 2: NBO Analysis of the H-Bonded Complexes of Rare-Gas FRgH Compounds (Rg = He, Ar, and Kr) Including NBO Charges (i.e., at F, Rg, and H), Polarization of Rg−H Bond, Population of σ*(Rg−H), the Energies of n(F) → σ*(X−H) and n(Y) → σ*(X−H) Interactions, and Total Binding Energies of the Complexes at the MP2 Level with 6-311++G(d,p) and 6-311++G(2d,2p) Basis Sets[a]

FRgH···Y	MP2/BS BS	q_F, a.u.	q_{Rg}, a.u.	q_H, a.u.	Pol (Rg−H), % at Rg	Pop σ* (Rg−H)	$E_{n→σ*}$, kcal/mol[b]	$E'_{n→σ*}$, kcal/mol[c]	E_{int} (ZPE), kcal/mol[d]
Rg = He	6-311++G(d,p)	−0.6472	0.3289	0.3182	81.58	0.1971	81.59		−
Y = none	6-311++G(2d,2p)	−0.6842	0.3353	0.3489	81.05	0.1747	73.58	−	−
Rg = He	6-311++G(d,p)	−0.7211	0.3340	0.3815	80.56	0.1579	54.59	2.63	1.0 [1.0]
Y = OC	6-311++G(2d,2p)	−0.7896	0.3360	0.4351	81.95	0.1544	48.85	9.74	1.3 [1.4]
Rg = He	6-311++G(d,p)[e]	−0.9720	0.1393	0.2999	−	−	−	−	16.5[15.1]
Y = CO	6-311++G(2d,2p)[e]	−0.9639	0.1545	0.3010	−	−	−	−	15.0 [13.4]
Rg = He	6-311++G(d,p)	−0.9041	0.2933	0.4534	83.17	0.1870	23.89	86.28	4.5 [4.3]
Y = N₂	6-311++G(2d,2p)	−0.8784	0.3103	0.4587	83.07	0.1552	26.65	70.20	4.9 [4.8]
Rg = He	6-311++G(d,p)[e]	−0.8663	0.2396	0.3047	−	−	−	−	5.8 [5.3]
Y = P₂	6-311++G(2d,2p)	−0.8422	0.2778	0.3686	83.83	0.2639	25.84	96.73	5.5 [5.3]
Rg = He	6-311++G(d,p)[e]	−0.9799	0.1335	0.5304	−	−	−	−	37.2 [35.0]
Y = OH₂	6-311++G(2d,2p)	−0.9754	0.1389	0.5259	−	−	−	−	33.6 [31.7]
Rg = Ar	6-311++G(d,p)	−0.7738	0.5530	0.2208	68.65	0.1093	32.42	−	−
Y = none	6-311++G(2d,2p)	−0.7614	0.5358	0.2257	68.12	0.1088	38.08	−	−
Rg = Ar	6-311++G(d,p)	−0.8128	0.5586	0.2514	69.41	0.0933	30.54	1.49	0.8 [0.9]
Y = OC	6-311++G(2d,2p)	−0.7909	0.5371	0.2507	69.09	0.0969	33.55	1.68	0.8 [1.0]
Rg = Ar	6-311++G(d,p)	−0.8808	0.5087	0.2618	71.73	0.1575	19.62	51.03	4.5 [4.7]
Y = CO	6-311++G(2d,2p)	−0.8414	0.4927	0.2644	71.18	0.1439	24.82	37.90	4.4 [4.2]
Rg = Ar	6-311++G(d,p)	−0.8360	0.5485	0.2691	69.94	0.0942	26.14	6.38	2.5 [2.4]
Y = N₂	6-311++G(2d,2p)	−0.8059	0.5259	0.2642	69.56	0.0989	31.28	6.32	1.9 [2.0]
Rg = Ar	6-311++G(d,p)	−0.8291	0.5249	0.2408	70.72	0.1361	26.41	19.09	3.1 [2.9]
Y = P₂	6-311++G(2d,2p)	−0.8014	0.5046	0.2390	70.35	0.1378	30.34	18.52	2.8 [2.6]
Rg = Kr	6-311++G(d,p)	−0.7514	0.6506	0.1008	60.99	0.1439	48.64	−	−
Y = none	6-311++G(2d,2p)	−0.7591	0.6516	0.1075	61.02	0.1222	48.62	−	−
Rg = Ar	6-311++G(d,p)[e]	−0.9747	0.2923	0.4231	−	−	−	−	18.6 [17.1]
Y = OH₂	6-311++G(2d,2p)	−0.9646	0.2676	0.4330	−	−	−	−	15.5 [14.3]
Rg = Kr	6-311++G(d,p)	−0.7648	0.6505	0.1138	61.76	0.1192	46.75	0.54	0.6 [0.5]
Y = OC	6-311++G(2d,2p)	−0.7732	0.6514	0.1202	61.79	0.1134	45.41	0.82	0.9 [0.6]
Rg = Kr	6-311++G(d,p)	−0.7815	0.6321	0.1317	62.35	0.1253	43.92	6.02	2.2 [1.9]
Y = CO	6-311++G(2d,2p)	−0.7935	0.6276	0.1378	62.71	0.1242	41.30	9.94	2.4 [2.2]
Rg = Kr	6-311++G(d,p)	−0.7719	0.6432	0.1239	61.83	0.1190	45.58	1.86	1.3 [1.3]
Y = N₂	6-311++G(2d,2p)	−0.7786	0.6440	0.1284	61.92	0.1142	44.50	2.22	1.3 [1.4]
Rg = Kr	6-311++G(d,p)	−0.7664	0.6393	0.1152	61.94	0.1275	46.16	3.26	1.7 [1.5]
Y = P₂	6-311++G(2d,2p)	−0.7554	0.6368	0.1175	62.11	0.1280	44.40	5.95	1.8 [1.6]
Rg = Kr	6-311++G(d,p)	−0.8490	0.5905	0.2076	66.67	0.1147	28.37	27.52	7.4 [7.6]
Y = OH₂	6-311++G(2d,2p)	−0.8461	0.5935	0.2017	66.39	0.1121	28.69	26.79	7.0 [7.1]
Rg = Kr	6-311++G(d,p)[e]	−0.9825	0.1484	0.4035	−	−	−	−	31.1[29.7]
Y = NH₃	6-311++G(2d,2p)	−0.9758	0.1542	0.3973	−	−	−	−	29.3 [27.5]

[a] See the Supporting Information for the analogous DFT data, MP2 results with different basis sets and for uncorrected interaction energies. [b] E[n(F) → σ*(Rg−H)]. [c] E[n(Y) → σ*(Rg−H)]. [d] The values in square brackets are the interaction energies after BSSE correction. [e] Bond polarizations, orbital populations, and orbital interaction energies are unavailable due to the change in the dominant NBO structure.
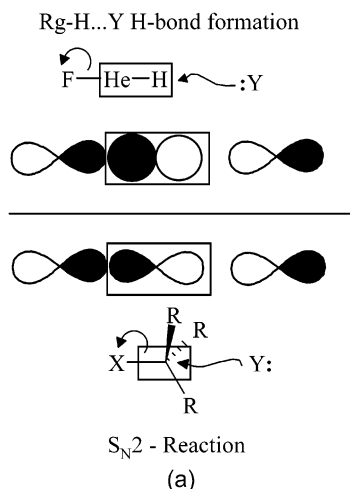
Rg-H...Y H-bond formation

S_N2 - Reaction

(a)

Figure 5. Analogy of F⁻···He···H−Y⁺ fragmentation of FHeH···Y complexes with an S_N2 reaction.

isoelectronic but differ significantly in charge distribution of the Y moiety (note, for example, the opposite dipole moments of CO and OC) as well as in donor ability of its lone pair participating in the n(Y) → σ*(H−Rg) hyperconjugative

interaction. These differences are reflected in the observed structural effects.

Although the structures of free hypervalent F−Rg−H molecules are quite sensitive to the level of theory,[37] formation of H-bonds in these systems always leads to elongation of the F−Rg bonds. In contrast, the Rg−H bonds may be either contracted or elongated depending on the nature of the H-bond acceptor Y and the level of theory used for the computation. For the weakest hyperconjugative donor, the oxygen lone pair of carbon monoxide, significant Rg−H bond contraction is observed in all cases. In the intermediate case (Y = N₂), a much smaller Rg−H bond contraction is found for Rg = He. In the case of the carbon lone pair of CO (the strongest donor), a significant Rg−H bond *elongation* is found in F−He−H···CO complex,[38] whereas the complexes with Rg = Ar and Kr remain blue-shifted. The H···Y distances also vary significantly depending on the nature of X and the quality of the basis set (from 1.2 to 2.2 Å for FHeH). In general, shorter H···Y distances correspond to a larger Rg−F bond elongation.

The role of the acceptor ability of σ*(Rg−H) orbitals in H-bonding is further illustrated by comparing FRgH···OH₂ complexes. The oxygen lone pair serves as a relatively strong hyperconjugative donor in the n(O) → σ*(H−Rg) interaction

Hypervalent Rare-Gas FRg−H···Y Sandwiches

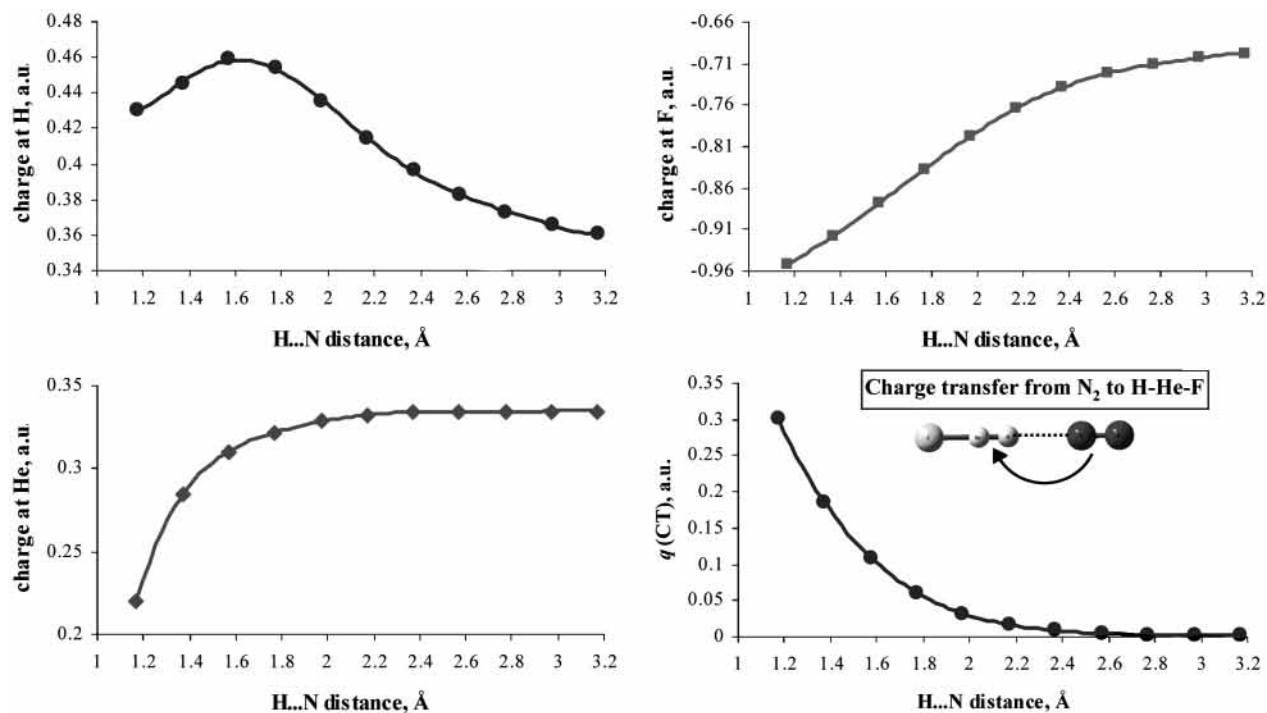*J. Phys. Chem. A, Vol. 108, No. 21, 2004* **4725**

Figure 6. Correlations of H···N bond length in FHeH···N_2 complex with the charges at H, F, and He as well as with the magnitude of net charge transfer from N_2 to H−He−F moiety at the MP2/6-311++G(2d,2p) level.
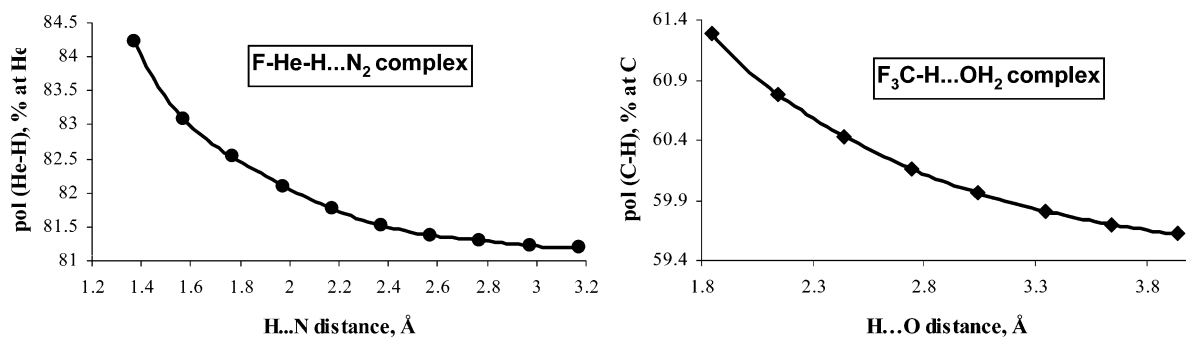

Figure 7. Correlations of H···Y distance in FHeH···N_2 and F_3C−H···OH_2 complexes with the corresponding polarizations of He−H (MP2/6-311++G(2d,2p) level) and C−H bonds.[7]

which leads to the H−Rg bond elongation in Rg = He and Ar complexes. Still, in the case of the weaker acceptor, σ*(Kr−H) orbital, Rg−H bond contraction and blue shift are observed. An ever stronger donor, the nitrogen lone pair of ammonia, is needed to provide "deprotonation" of FKrH with concomitant Kr−H bond elongation. These effects illustrate how the nature of H-bonding in these systems (red- vs blue-shift) depends on a rather complicated interplay of the electronic factors.

Electronic Changes Associated with H-Bond Formation in F−Rg−H···Y Systems. Independent of the initial atomic charges and polarization,[39] H-bond formation increases Rg−H bond polarization and positive charge on H atoms, changes which are analogous those observed during H-bond formation involving 2e-2c bonds. These effects are significant; for example, the positive charges on He and H atoms are almost equal in the isolated FHeH molecule, whereas the H atom has 50% more of the positive charge in the FHeH···N_2 complex.

The above data further illustrate that the original premise of our repolarization/rehybridization model of blue-shifted H-bonding is fully applicable to hypervalent systems and that repolarization continues to serve as the key factor in the electronic readjustments during the process of blue-shifted H-bond formation. In classic σ(X−H) bonds, repolarization is

translated into structural changes through rehybridization whereas in the intrinsically highly polarizable but inimical to rehybridization 3c,4e X−H bonds the structural reorganization is achieved through rebalancing the contributions from individual VB structures corresponding to the competing n → σ*(Rg−H) interactions.

Although the initial charge distribution is different in the three FRgH molecules in Table 2,[40] all Rg−H bonds are still polarized toward the rare gas atom. Due to the strong polarization of σ*(Rg−H) orbitals toward H, the hydrogen ends of these orbitals are stronger hyperconjugative acceptors than their rare gas termini. The most highly polarized He−H bond (>80% at He) is the strongest hyperconjugative acceptor among the Rg−H bonds, FHeH is the strongest Brönsted acid among the three FRgH compounds and, thus, it is more likely to permanently transfer a proton to the lone pair of H-bond acceptor Y (vide infra). In accord with this notion, a very short N−H distance (∼1.2 Å) is found for the F−He−H···CO complex whereas the He−H distance is *increased* and a *red-shifted* H-bond is formed. In this case, the n(C) → σ*(He−H) interaction is evidently so large that the proton formally shifts to the F⁻···He···[HCO⁺] structure, breaking (and red-shifting) the formal He−H bond. These dramatic electronic rearrangements suggest that FHe-
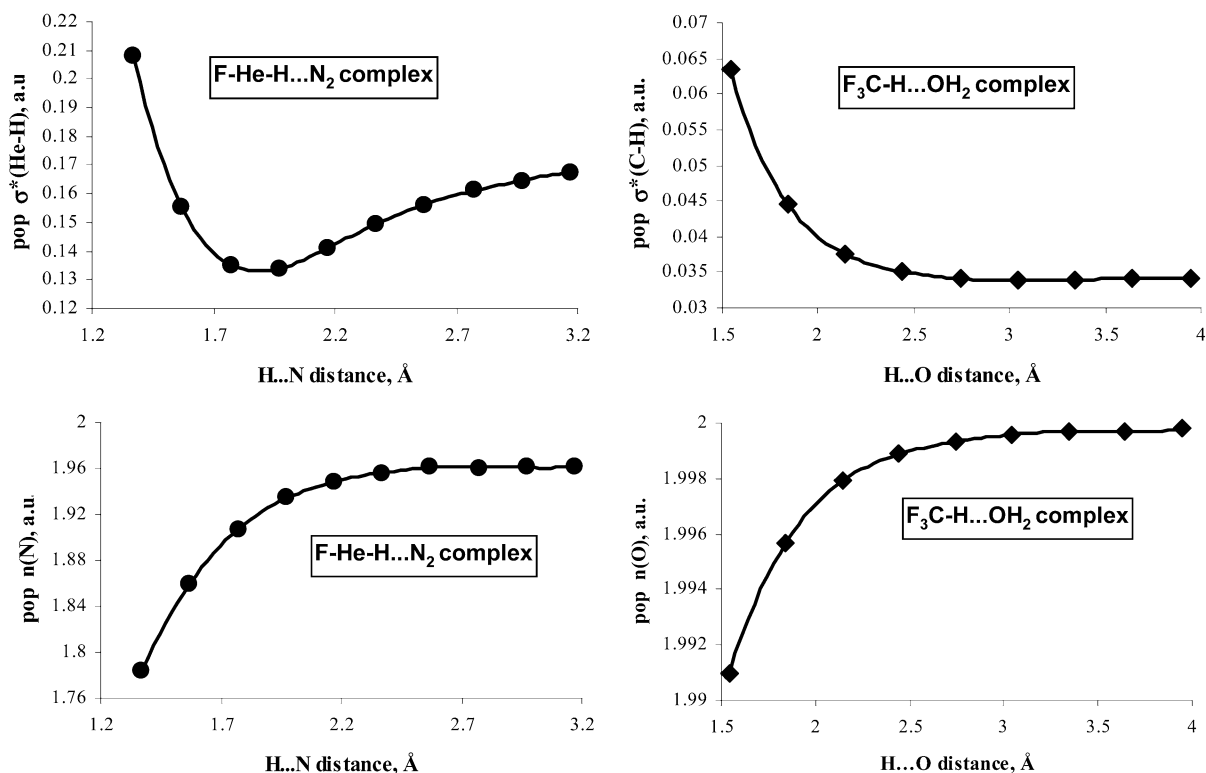
Figure 8. Correlations of the H⋯Y distance with the populations of $\sigma^*(X-H)$ and n(Y) orbitals in $F-He-H\cdots N_2$ (MP2/6-311++G(2d,2p) level) and $F_3C-H\cdots OH_2{}^7$ complexes.

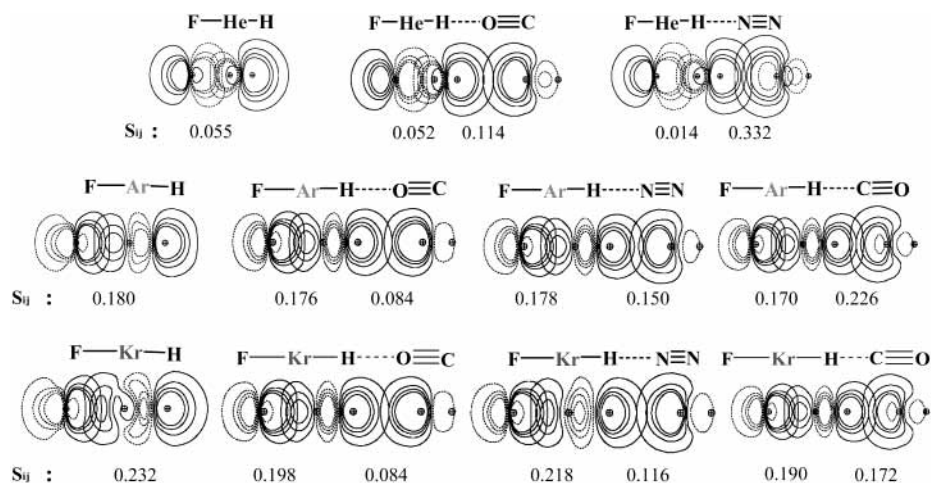**Figure 9.** NBO plots for two hyperconjugative interactions such as n(F) → $\sigma^*(Rg-H)$ in the monomer as well as in the complex and n(Y) → s*(Rg-H) in the complex along with the overlap elements S_{ij} (a.u.) for the corresponding interactions (MP2/6-311++G(d,p) level) (Fock matrix elements and energies of the corresponding interactions are given in the Supporting Information).

H⋯Y is a highly unstable system, with hair-trigger sensitivity to small variations in the Lewis base strength of the incoming ligand Y.[41] This notion is further supported by the smaller magnitude of the blue shift in the $F-He-H\cdots N_2$ complex compared with the analogous complexes of HArF and HKrF.

Finally, an interesting feature of the $F-He-H\cdots OC$ and $F-Ar-H\cdots OC$ complexes is that *both* hydrogen and rare gas atoms become more electropositive and that the change in polarization of the respective Rg–H bond is smaller than in other complexes. This is not surprising because the lone pair of the formally sp-hybridized oxygen atom is an unusually poor electron donor. This is confirmed by the rather low energies of hypervalent n(O) → $\sigma^*(He-H)$ interactions, more than an order of magnitude lower than in the case of n(C) → $\sigma^*(He-H)$ interaction in $F-He-H\cdots CO$ complex. Differences in the orbital overlaps given in Figure 9 further illustrate how the competition

of two hyperconjugative donors for a $\sigma^*(Rg-H)$ acceptor leads to a transition of "He-bonding" to H-bonding depending on the nature of the donor and the acceptor. Again, FRgH⋯OC complexes are somewhat unusual.

Most importantly, all major effects reported in the previous section are still present in the systems discussed in the present section, as the H-bonds are formed, H becomes more electropositive, fluorine becomes more negative, $\sigma(Rg-H)$ becomes more polarized, the n(F) → $\sigma^*(Rg-H)$ interaction gets weaker, and the covalent F–Rg bond order decreases. In addition, in those cases when blue-shifted H-bonds are formed, the population of the $\sigma^*(Rg-H)$ orbital decreases and the covalent H–Rg bond order increases.

Binding Energies. Although the balance between the dominant hyperconjugative interactions is important for understanding structural and electronic changes associated with formation of
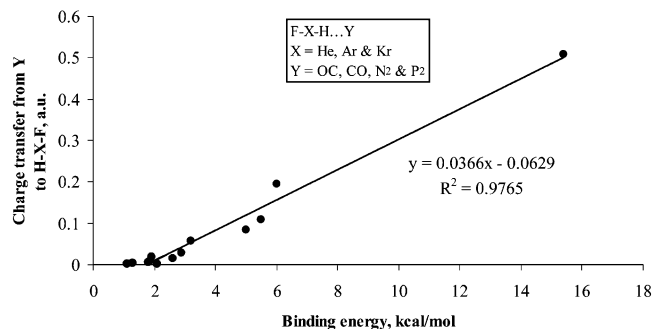
Hypervalent Rare-Gas FRg−H···Y Sandwiches

J. Phys. Chem. A, Vol. 108, No. 21, 2004 **4727**

Figure 10. Correlation of the amount of electronic charge transferred from Y to F−Rg−H moiety with the binding energies of the FRgH···Y complexes.
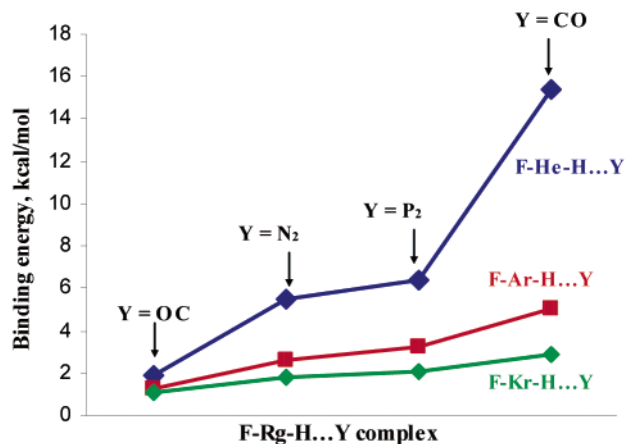

Figure 11. Trends in relative binding energies in the FRgH···Y complexes.

weakly bound (and blue-shifted) complexes, the n(Y) → σ*(H−Rg) charge transfer plays a dominant role in determining the binding energies of the strongly bound red-shifted complexes (Figure 10). Figure 11 further illustrates how the relative binding energies are determined by the interplay of two factors: the acceptor ability of σ*(H−Rg) orbitals (He>Ar>Kr) and the donor ability of lone pairs of Y (CO>P$_2$>N$_2$>OC). As the magnitude of the n(Y) → σ*(H−Rg) interaction increases, the binding energy increases, at first slowly but more rapidly accompanied by a more pronounced structural and electronic reorganization as the hyperconjugative n(Y) → σ*(H−Rg) energies become larger.[42]

Natural Resonance Theory (NRT) Analysis of Hypervalency and Electronic Structures of F−Rg−H···Y Complexes. It has been suggested that chemical bonding in XRgH compounds can to a first approximation be treated as an X$^-$ [RgH]$^+$ ion pair within the frame of simple ionic model[43] and further refined in VB terms "as a resonance hybrid between several possible structures from which the most important is HRg$^+$X$^-$".[43] In particular, Lignell and co-workers noted that complexation of the HRgF molecules with N$_2$ leads to increased charge separation of the [HRg]$^+$X$^-$ type and "as a result, the HRg moiety structurally approaches the [HRg]$^+$cation". McDowell provided further support for this notion[10a] but also reported an example of a red-shifted FRgH···Y, Y = P$_2$ complex.[10]

Three structures are of primary importance for hypervalent binding in the FHeH moiety: F$^-$ [Rg−H]$^+$, nucleophilic F$^-$ attack on Rg−H+ ion, (I); [F−Rg]$^+$H$^-$, nucleophilic H$^-$ attack on Rg-F+ ion, (II); and F$^-$[Rg]H$^+$, ionic F(−)··[He]··H(+) sandwich with ionic F(−)··H(+) long bond (III) (compare with Figure 1).[44] All structures include aspects of ionic and covalent interactions, but only structure I has covalent Rg−H character

and, thus, is the most important for studying the Rg−H···Y blue-shifting phenomenon. Note, however, that resonance structure III may gain importance for stronger donors and lead to complete proton transfer to the donor with concomitant liberation of Rg atom and fluoride anion.

As a result, the hypervalency presents these complexes with an entirely new "mechanism" to strongly enhance the n(Y) → σ*(He−H) interaction without benefit of rehybridization. It is apparent that although the first (fluoridic) resonance structure can H-bond appreciably the second (hydridic) form presents only a nonbonded H(−) Lewis base to the incoming Y that offers no possibility for the characteristic n(Y) → σ*(He−H) interaction. Formation of the FHeH···Y H-bond must therefore be accompanied by a strong increase in the weighting of the fluoridic resonance structure, with a corresponding increase in the He−H bond order and resultant He−H shortening and blue-shifting.

The changes in the relative weights of the dominant VB configurations lead to increased charge separation of the [HRg]$^+$X$^-$ type as "the HRg moiety structurally approaches the [HRg]$^+$cation"[13] and provide an efficient mechanism for the structural changes which is not readily available in classic 2e,2c bonds but serves the same purpose as rehybridization in the classic systems: formation of X−H···Y H-bonds increases effective electropositivity of hydrogen and leads to additional polarization of X−H bonds.

To illustrate this mechanism in more detail, let us analyze the changes during H-bond formation in the FHeH···N$_2$ complex using the NRT analysis which provides a more detailed description on the nature of binding in hypervalent FRgH compounds including the relative weights of important VB structures.[45]

In agreement with the above model, the covalent FHe bond order vanishes, whereas the ionic FHe bond order reaches unity as the FHeH···N$_2$ complex is formed. Changes in the HeH bond order display a more complicated pattern due to the interplay of several effects and the contributions of different VB structures of varying weights. At H···N distances of 2−2.5 Ang, the covalent H−He bond order increases compared to that in the isolated FHeH indicating the "blue-shifted region", but at the "red-shifted" region corresponding to the shorter H···N distances, the H−He bond order progressively decreases.

The role of covalent He−H bond order in determining the He−H bond length is illustrated by Figure 13. In the blue-shifted complexes, the covalent He−H bond order is slightly larger than in the bare FHeH molecule, but in the red-shifted FHeH···CO complex, the covalent He−H bond order is dramatically decreased.[46]

Conclusion

Repolarization of X−H bonds during the process of X−H···Y H-bond formation can lead to X−H bond shortening and the blue shift of the corresponding IR stretching frequency via two mechanisms: (a) rehybridization in the case of classic 2c,2e bonds and (b) rebalancing of relative contributions of different VB structures in the case of hypervalent 3c,4e bonds. The second mechanism increases the weight of the F$^-$ [Rg−H]$^+$ resonance and decreases the weight of the [F−Rg]$^+$ H$^-$ resonance leading to an increased [Rg−H] cation character of the Rg−H moiety. The F−Rg−H···Y complexes can be best described as a F$^-$···Rg−H$^+$···Y sandwich of a positively charged diatomic cation [He−H]$^+$ with two hyperconjugative donors, whereas the process of H-bond formation presents a compromise between the loss of the n(F) → σ*(Rg−H)
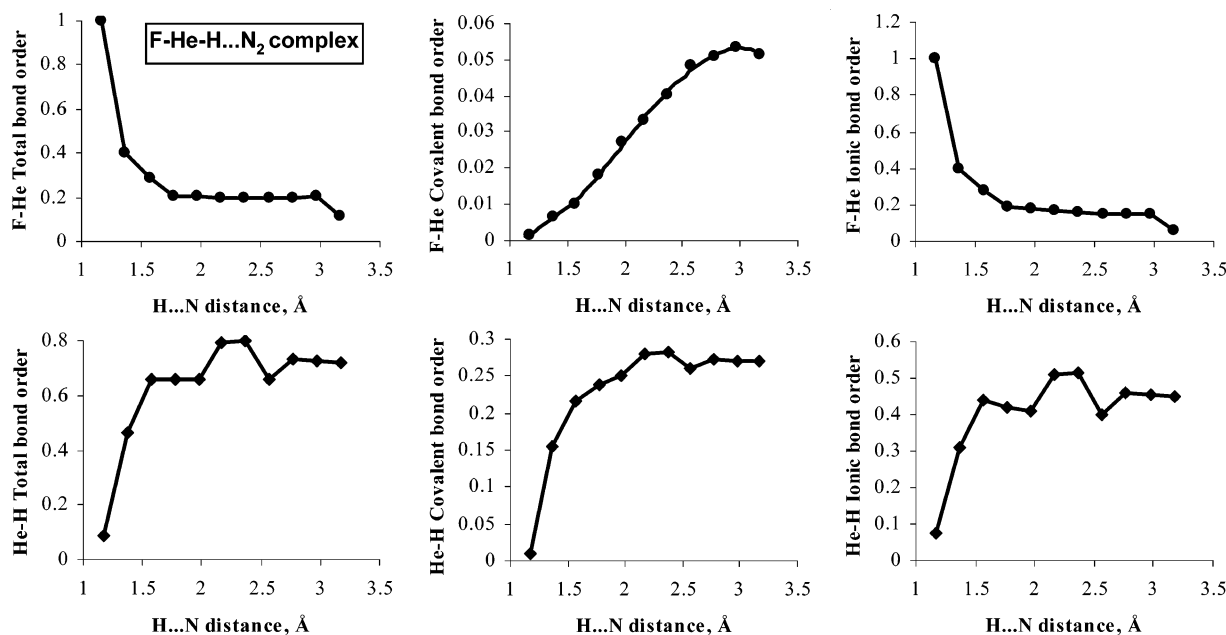
Figure 12. Changes in covalent, ionic, and total He−H and F−He bond orders upon decrease in H···N distance lengths with He−H covalent bond order in the FHeH···N$_2$ complex.
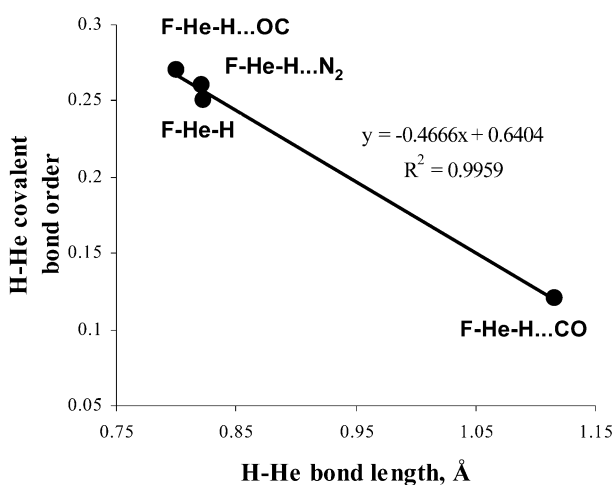

Figure 13. Correlation of He−H bond lengths with He−H covalent bond order in the FHeH···Y complexes.

interaction (with concomitant *increase* in Rg−H covalent bonding and blue-shift of Rg−H stretching frequency) and gain in the n(N) → σ*(H−Rg) interaction and covalent Y−H bonding (with concomitant *decrease* in Rg−H covalent bonding and the red-shift of Rg−H stretching frequency).

Supporting Information Available: Geometries and absolute energies for all molecules and complexes in this paper. Tables with structural parameters and NBO analysis of H-bonded complexes the MP2 level with cc-pVTZ and cc-pVDZ basis sets. NBO analysis of the H-bonded complexes at the B3LYP level with several basis sets. Changes in the bond lengths and NBO quantities upon stretching the H···N bond in FHeH···N$_2$ complex at the MP2/cc-pVTZ and MP2/6-311+G-(2d,2p) levels. Changes in the NRT bond orders upon stretching the H···N bond of the H-bonded FHeH···N$_2$ complex at the

MP2/6-311+G(2d,2p) level. The interaction energies for the H-bonded complexes at the MP2 level with 6-311++G(d,p) and 6-311++G(2d,2p) basis sets. The correlations of H···N bond length in FHeH···N$_2$ complex with the F−He and He−H bond lengths and with the polarization of He in He−H bond (MP2/cc-pVTZ level). The correlations of H···N bond length in FHeH···N$_2$ complex with natural charges at H, F and He atoms and with the amount of charge transferred from N$_2$ to H−He−F moiety (MP2/cc-pVTZ level). The correlations of H···Y bond length in FXH···Y (X = He, Ar, Kr and Y = N$_2$, CO, OC and P$_2$) complexes with their binding energies calculated at the MP2/6-311+G(2d,2p) level. NBO plots for selected hyperconjugative interactions in monomers and in complexes along with the NBO deletion energies (kcal mol^{-1}) and Fock matric-F$_{ij}$ (kcal mol^{-1}) elements for the corresponding interactions (MP2/6-311++G(d,p) level). This material is available free of charge via the Internet at http://pubs.acs.org.

References and Notes

(1) Hobza, P.; Havlas, Z. *Chem. Rev.* **2000**, *100*, 4253.

(2) Buděšinsky, M.; Fiedler, P.; Arnold, Z. *Synthesis* **1989**, 858. Boldeskul, I. E.; Tsymbal, I. F.; Ryltsev, E. V.; Latajka, Z.; Barnes, A. J. *J. Mol. Struct.* **1997**, *436*, 167.

(3) Hobza, P.; Špirko, V.; Havlas, Z.; Buchhold, K.; Reimann, B.; Barth, H.-D.; Brutschy, B. *Chem. Phys. Lett.* **1999**, *299*, 180. Reimann, B.; Buchhold, K.; Vaupel, S.; Brutschy, B.; Havlas, Z.; Hobza, P. *J. Phys. Chem. A* **2001**, *105*, 5560.

(4) Experimental Evidence for the Blue-Shifting X−H···Y Hydrogen Bonding. van der Veken, B. J.; Herrebout, W. A.; Szostak, R.; Shchepkin, D. N.; Havlas, Z.; Hobza, P. *J. Am. Chem. Soc.* **2001**, *123*, 12290. Delanoye, S. N.; Herrebout, W. A.; van der Veken, B. J. *J. Am. Chem. Soc.* **2002**, *124*, 7490. Delanoye, S. N.; Herrebout, W. A.; van der Veken, B. J. *J. Am. Chem. Soc.* **2002**, *124*, 11854. Matsuura, H.; Yoshida, H.; Hieda, M.; Yamanaka, S.; Harada, T.; Shin-ya, K.; Ohno, K. *J. Am. Chem. Soc.* **2003**, *125*, 13910.

(5) Hobza, P.; Špirko, V.; Selzle, H. L.; Schlag, E. W. *J. Phys. Chem. A* **1998**, *102*, 2501. Hobza, P.; Havlas, Z. *Chem. Phys. Lett.* **1999**, *303*, 447.

(6) (a) Li, X.; Liu, L.; Schlegel, H. B. *J. Am. Chem. Soc.* **2002**, *124*, 9639. (b) Hermansson, K. *J. Phys. Chem. A* **2002**, *106*, 4695. Pejov, L.; Hermansson, K. *J. Chem. Phys.* **2003**, *119*, 313. (c) Gu, Y.; Kar, T.; Scheiner, S. *J. Am. Chem. Soc.* **1999**, *121*, 9411. Scheiner, S.; Grabowski, S. J.; Kar, T. *J. Phys. Chem. A* **2001**, *105*, 10607. Scheiner, S.; Kar, T. *J. Phys. Chem. A* **2002**, *106*, 1784. (d) Cubero, E.; Orozco, M.; Hobza, P.;

Hypervalent Rare-Gas FRg−H···Y Sandwiches

J. Phys. Chem. A, Vol. 108, No. 21, 2004 **4729**

Luque, F. J. *J. Phys. Chem. A* **1999**, *103*, 6394. (e) Masunov, A.; Dannenberg, J. J.; Contreras, R. H. *J. Phys. Chem. A* **2001**, *105*, 4737. (f) Liu, S. Y.; Dykstra, C. E.; Malik, D. J. *Chem. Phys. Lett.* **1986**, *130*, 403.46. Liu, S.; Dykstra, C. E. *J. Phys. Chem.* **1986**, *90*, 3097. Liu, S. Y.; Dykstra, C. E. *Chem. Phys. Lett.* **1987**, *136*, 22. Dykstra, C. E. *Acc. Chem. Res.* **1988**, *21*, 355. Parish, C. A.; Dykstra, C. E. *J. Phys. Chem.* **1993**, *97*, 9374. (g) Qian, W.; Krimm, S. *J. Phys. Chem. A* **2002**, *106*, 6628. (h) Karpfen, A.; Kryachko, E. S. *J. Phys. Chem. A* **2003**, *107*, 9724. (i) Wysokinski, R.; Michalska, D.; Bienko, D. C.; Zeegers-Huyskens, T. *J. Phys. Chem. A* **2003**, *107*, 8730.

(7) Alabugin, I. V.; Manoharan, M.; Peabody, S.; Weinhold, F. *J. Am. Chem. Soc.* **2003**, *125*, 5973.

(8) Presence of a suitable mechanism for translation of repolarization into structural changes is important, when molecular structure inhibits rehybridization, only the classic red-shift H-bonding is observed even for weakly acceptor X−H bonds.

(9) Bent, H. A. *Chem. Rev.* **1961**, *61*, 275.

(10) (a) A computational study of hydrogen-bonded complexes of HKrCl: N₂···HKrCl, CO···HKrCl, HF···HKrCl. McDowell, S. A. *J. Chem. Phys.* **2003**, *119*, 3711. (b) Comparison of the intermolecular properties of N₂···HArF with N₂···HF. McDowell, S. A. *J. Chem. Phys.* **2003**, *118*, 4066. (c) Blue-shifting hydrogen bonding in FKrH···N₂: McDowell, S. A. *J. Chem. Phys.* **2003**, *118*, 7283. (d) A computational study of the HArF···CO: McDowell, S. A. *Chem. Phys. Lett.* **2003**, *368*, 649. (e) Intermolecular complexes of HArF and HF. McDowell, S. A. *Chem. Phys. Lett.* **2003**, *377*, 143. (f) Blue shifting and red shifting hydrogen bonds: HArF···N₂ and HArF···P₂ complexes. McDowell, S. A. *Phys. Chem. Phys.* **2003**, *5*, 808. (g) Blue-shifting hydrogen bonding in the ClArH···N₂ complex. *J. Mol. Struct. THEOCHEM* **2003**, *625*, 243.

(11) Large blueshift of the H−Kr stretching frequency of HKrCl upon complexation with N₂. Lignell, A.; Khriachtchev, L.; Pettersson, M.; Räsänen, M. *J. Chem. Phys.* **2002**, *117*, 961.

(12) Wang, J.-T.; Feng, Y.; Liu, L.; Li, X.-S.; Guo, Q.-X. *Chem. Lett.* **2003**, *32*, 746.

(13) Matrix-isolation and ab initio study of HArF···N₂, HKrF···N₂ and HKrCl···N₂. Lignell, A.; Khriachtchev, L.; Pettersson, M.; Räsänen, M. *J. Chem. Phys.* **2003**, *118*, 11120.

(14) (a) Lewis, *G. N. J. Am. Chem. Soc.* **1916**, *38*, 762. (b) Langmuir, J. *J. Am. Chem. Soc.* **1919**, *41*, 868.

(15) Coulson, C. A. *J. Chem. Soc.* **1964**, 1442. Musher, J. I. *Angew. Chem., Int. Ed. Engl.* **1969**, *8*, 54.

(16) For recent discussions, see: Noury, S.; Silvi, B.; Gillespie, R. J. *Inorg. Chem.* **2002**, *41*, 2164. Dobado, J. A.; Martinez-Garcia, H.; Molina, J. M.; Sundberg, M. R. *J. Am. Chem. Soc.* **1999**, *121*, 3156.

(17) For interesting alternative approaches, see: Dobado, J. A.; Martinez-Garcia, H.; Molina, J. M.; Sundberg, M. R. *J. Am. Chem. Soc.* **1999**, *121*, 3156. Ponec, R.; Girones, X. *J. Phys. Chem. A* **2002**, *106*, 9506.

(18) The octet rule and hypervalence: Gillespie, R. J.; Silvi, B. *Coord. Chem. Rev.* **2002**, *233−234*, 53. Application of 3c,4e bonding to main group hypervalent molecules in context of the octet rule. Cheung, Y.-S.; Ng, C.-Y.; Chiu, S.-W.; Li, W.-K. *J. Mol. Struct. THEOCHEM* **2003**, *623*, 1.

(19) Pauling, L. *The Nature of the Chemical Bond*; Cornell University Press: Ithaca, NY, 1948. Coulson, C. A. *Valence*; Clarendon: Oxford, U.K., 1952. Kwart, H.; King, K. G. *d-Orbitals in the Chemistry of Silicon, Phosphorus and Sulfur*; Springer: Berlin, 1977; and references therein.

(20) For example, including d orbitals on sulfur is important for accurate description of electronic structure of SF₆ because these orbitals allow strong back transfer from the negatively charged F ligands to the strongly positively charged (+2.9e) S atom greatly increasing molecular stability. Reed, A. E.; Weinhold, F. *J. Am. Chem. Soc.* **1986**, *108*, 3586.

(21) Hach, R. J.; Rundle, R. E. *J. Am. Chem. Soc.* **1951**, *73*, 4321.

(22) Pimentel, G. C. *J. Chem. Phys.* **1951**, *19*, 446.

(23) Bagus, P. S.; Liu, B.; Liskow, D. H.; Schaefer, H. F. *J. Am. Chem. Soc.* **1975**, *97*, 7216. Reed, A. E.; Weinhold, F. *J. Am. Chem. Soc.* **1986**, *108*, 8, 3586. Reed, A. E.; Schleyer, P. v. R. *J. Am. Chem. Soc.* **1990**, *112*, 1434. Magnusson, E. *J. Am. Chem. Soc.* **1990**, *112*, 7940−7951.

(24) Kutzelnigg, W. *Angew. Chem., Int. Ed. Engl.* **1984**, *23*, 272.

(25) Bilham, J.; Linnett, J. W. *Nature* **1964**, *201*, 1323.

(26) VB description of hypervalent bonding was successfully used for developing of Molecular Mechanics (MM) methods suitable for description of hypervalent molecules: Cleveland, T.; Landis, C. L. *J. Am. Chem. Soc.* **1996**, *118*, 6020.

(27) In addition, even when a superposition of the above Lewis structures is considered, the bond hybridization concept is of little use for description of ionic bonding, such as between F⁻ and [Xe−F]⁺ in such partial Lewis structures. For example, He−H bond in an isolated FHeH molecule has ionic bond order of 0.38 and covalent bond order of only 0.25 at the MP2/6-311++G** level (vide infra). VB-interpretation of this bonding situation in terms of s- and p-character in the bonding orbitals is not straightforward. Note, however, that Munzarova and Hoffman shown recently how to incorporate changes in s-character in the general MO picture of three-center

bonding. Munzarova, M. L.; Hoffmann, R. *J. Am. Chem. Soc.* **2002**, *124*, 4787.

(28) Frisch, M. J.; Trucks, G. W.; Schlegel, H. B.; Scuseria, G. E.; Robb, M. A.; Cheeseman, J. R.; Zakrzewski, V. G.; Montgomery, J. A., Jr.; Stratmann, R. E.; Burant, J. C.; Dapprich, S.; Millam, J. M.; Daniels, A. D.; Kudin, K. N.; Strain, M. C.; Farkas, O.; Tomasi, J.; Barone, V.; Cossi, M.; Cammi, R.; Mennucci, B.; Pomelli, C.; Adamo, C.; Clifford, S.; Ochterski, J.; Petersson, G. A.; Ayala, P. Y.; Cui, Q.; Morokuma, K.; Malick, D. K.; Rabuck, A. D.; Raghavachari, K.; Foresman, J. B.; Cioslowski, J.; Ortiz, J. V.; Stefanov, B. B.; Liu, G.; Liashenko, A.; Piskorz, P.; Komaromi, I.; Gomperts, R.; Martin, R. L.; Fox, D. J.; Keith, T.; Al-Laham, M. A.; Peng, C. Y.; Nanayakkara, A.; Gonzalez, C.; Challacombe, M.; Gill, P. M. W.; Johnson, B. G.; Chen, W.; Wong, M. W.; Andres, J. L.; Head-Gordon, M.; Replogle, E. S.; Pople, J. A. *Gaussian 98*, revision A.1; Gaussian, Inc.: Pittsburgh, PA, 1998.

(29) Boys, S. F.; Bernardi, F. *Mol. Phys.* **1970**, *19*, 553.

(30) Glendening, E. D.; Badenhoop, J. K.; Reed, A. E.; Carpenter, J. E.; Weinhold, F. F. *NBO 4.0*; Theoretical Chemistry Institute, University of Wisconsin: Madison, WI, 1996.

(31) Weinhold F. in Schleyer P.v. R., Ed. *Encyclopedia of Computational Chemistry*; Wiley: New York, 1998; Vol. 3, p 1792.

(32) Reed, A. E.; Weinhold, F. *J. Chem. Phys.* **1985**, *83*, 1736.

(33) Strasser, D.; Bhushan, K. G.; Pedersen, H. B.; Wester, R.; Heber, O.; Lafosse, A.; Rappaport, M. L.; Altstein, N.; Zajfman, D. *Phys. Rev. A* **2000**, *61*, 060705/1 and references therein. Glockler, G.; Fuller, D. L. *J. Chem. Phys.* **1933**, *1*, 886. Bishop, D. M.; Cheung, L. M. *J. Mol. Spectrosc.* **1979**, *75*, 462. Green, T. A.; Michels, H. H.; Browne, J. C. *J. Chem. Phys.* **1978**, *69*, 101 and references therein.

(34) For a more general discussion of the nature of He bonding in diatomic cations HeX^{n+}, see: Frenking, G.; Koch, W.; Cremer, D.; Gauss, J.; Liebmann, J. F. *J. Phys. Chem.* **1989**, *93*, 3397.

(35) One has to make a comment about the quality of theoretical analysis and, in particular, about the accuracy of NBO analysis for these systems. First, the geometries and bonding energies of the hypervalent H-bonded complexes are highly sensitive to the level of theory used, especially to the size of the basis set. Second, the structures are intrinsically highly delocalized and thus, NBO analysis, which is based on a single dominant Lewis structure can provide, at best, a qualitative description of these systems with contributions from other resonance structures treated as second-order perturbation corrections. The magnitude of these corrections (E(2) − second-order perturbation energies) can be taken as a measure of delocalizations.

(36) Nemukhin, A. V.; Grigorenko, B. L.; Khriachtchev, L.; Tanskanen, H.; Pettersson, M.; Räsänen, M. A. *J. Am. Chem. Soc.* **2002**, *124*, 10706.

(37) All calculated geometries are sensitive to the size of basis set but the sensitivity dramatically decreases in the order of He > Ar > Kr. Despite these differences, the trends for all three rare gas elements in Table 1 (Rg = He, Ar, and Kr) are qualitatively the same, the largest 6-311++G(2d, 2p) basis set gives the shortest Rg−H distances, whereas the smallest cc-pVDZ basis set results in the longest Rg−H distances (see the Supporting Information). Interestingly, the trends for Rg-F bonds are almost exactly the opposite except that there is an inversion between cc-pVDZ and cc-pVTZ in the case of Ar and Kr.

(38) Interestingly, at MP2/cc-pVTZ and MP2/cc-pVDZ levels, the FHeH and FArH complexes with N₂ are blue-shifted. Even the F−Kr−H···P₂ complex is blue shifted when the MP2/6-311++G(d, p) basis set is used. More flexible basis set allows for more profound electronic reorganization as evidenced by significantly shorter H···P distances and by considerably larger changes in the NBO charges in the F−Rg−H triade (vide infra). This frontier case where a switch from blue-shifted to red-shifted H-bonding depends on a combination of subtle factors and should provide an interesting case for a further study.

(39) Not surprisingly, formation of this complex is also accompanied by the most dramatic elongation of the Rg−F bond.

(40) Again, size of the basis set plays an important role: H becomes significantly more positive, and F is much more negative when a more extended basis set is used (Table 2 and the Supporting Information). The basis set effects are especially important for FHeH···Y systems. Treatment of the systems FRgH···Y complexes as [Rg−H]⁺ moiety sandwiched between F⁻ and N₂ donors (Figure 9) can rationalize these effects. For example, there is a large difference between structures of F−He−H···N₂ at MP2/6-311++G** (Table 2) and MP2/cc-pVTZ (Supporting Information) levels. At the first level, the He−H bond contraction is very small but He−F bond elongation is large, where the situation is just the opposite at the second level of theory. In accord with these structural changes, the balance between n(F) → σ*(He−H) and n(N) → σ*(H−He) interactions is changed for the two basis sets. Whereas at the MP2/6-311++G** level, the n(N) → σ*(H−He) interaction is dominant, and just the opposite is true at the MP2/cc-pVTZ level where n(F) → σ*(He−H) interaction is larger in magnitude. Remarkably, even despite these extreme differences in the electronic structures, the binding energy changes only from 5.2 to 2.5 kcal/mol for the two basis sets indicating a rather soft binding potential. Such intrinsic flexibility of these highly polarizable hypervalent assemblies is consistent with the remarkable ease of their electronic reorganization.

(41) The relative NBO charges at Rg and H (q_{Rg}/q_H) are 0.34/0.35 (Rg=He); 0.54/0.23 (Ar) and 0.65/0.10 (Kr).

(42) Such instability with respect to typical coordinating ligands no doubt affects the possibility of observing FHeH in common matrix conditions; for example, the dimerization interaction FHeH···FHeH may trigger spontaneous proton transfer and decomposition.

(43) Because the MP2 method is known to overestimate binding energies, we performed single-point computations of binding energies in three FRgH···N_2 complexes at CCSD(T)/6-311++G(2d, 2p)//MP2-6-311++G(2d, 2p) level of theory. The results were as follows (the MP2 data are given in parentheses in kcal/mol): F−He−H···N_2, 4.6 (5.2); F−He−H···N_2, 2.0 (2.6); F−He−H···N_2, 1.5 (1.8). These results illustrate that MP2 is adequate for the semiquantitative discussion in this paper which primarily focuses on the electronic structure of the complexes instead of the binding energies.

(44) Pettersson, M.; Lundell, J.; Räsänen, M. *Eur. J. Inorg. Chem.* **1999**, 729. See also: Last, I.; George, T. F. *J. Chem. Phys.* **1988**, *89*, 3071. Johns, J. W. C. *J. Mol. Spectrosc.* **1984**, *106*, 124. Warner, H. E.; Connor, W. T.; Woods, R. C. *J. Chem. Phys.* **1984**, *81*, 5413. Peterson, K. A.; Petrmichl, R. H.; McClain, R. L.; Woods, R. C. *J. Chem. Phys.* **1991**, *95*, 2352. **1982**, *21*, 4064. Klein, R.; Rosmus, P. *Z. Naturforsch.* **1984**, *39a*, 349.

(45) Interestingly, structure III, which corresponds to the n(He) formal lone pair, "encapsulated" by surrounding F(−) and H(+) ionic fragments sometimes is the leading NBO/NRT structure (for example, isolated FHeH species at the MP2/cc-pVDZ and B3LYP/BS (BS: 6-311++G**, cc-pVDZ, cc-pVTZ) levels). This structure has out-of-phase h(F)−h(H) character because any in-phase covalency, of σ(F−H) type, of these fragments would be strongly destabilized by unfavorable overlap (steric interactions) with the central n(He). So the lesser evil appears to be to use the out-of-phase σ*(F−H) combination that puts a node through n(He), thus avoiding this destabilization. Although it is unusual to see σ*(F−H) as the lower-energy occupied NBO, this is a consequence of the intruder He atom that occupies the usual bonding overlap region. In any event, this n(He)-σ*(HF) resonance structure contributes no He−H bond order.

(46) Glendening, E. D.; Weinhold, F. *J. Comput. Chem.* **1998**, *19*, 593. Glendening, E. D.; Weinhold, F. *J. Comput. Chem.* **1998**, *19*, 610. Glendening, E. D.; Badenhoop, J. K.; Weinhold, F. *J. Comput. Chem.* **1998**, *19*, 628.

(47) Problems with NRT analysis convergence of FRgH···Y complexes for Rg = Ar, Kr, and Xe were observed in accord with the multiconfigurational electronic wave function of these molecules. These analyses will be reported in the due course.